REPORT DOCUMENTATION PAGE

Form Approved
OMB No. 0704-0188

PLEASE DO NOT RETURN YOUR FORM TO THE ABOVE ADDRESS.

1. REPORT DATE *(DD-MM-YYYY)*	2. REPORT TYPE	3. DATES COVERED *(From - To)*
01-06-2004	Journal Article	2002 - 2003

4. TITLE AND SUBTITLE

Josephson junction triangular prism qubits coupled to a resonant LC bus.

5a. CONTRACT NUMBER

N/A

5b. GRANT NUMBER

N/A

5c. PROGRAM ELEMENT NUMBER

61102F

6. AUTHOR(S)

Stanford P. Yukon

5d. PROJECT NUMBER

2304

5e. TASK NUMBER

HE

5f. WORK UNIT NUMBER

2304HE03

7. PERFORMING ORGANIZATION NAME(S) AND ADDRESS(ES)

Electromagnetic Scattering Branch (AFRL/SNHE) Source Code: 437890
Electromagnetic Technology Division, Sensors Directorate
80 Scott Drive,
Hanscom AFB, MA 01731-2909

8. PERFORMING ORGANIZATION REPORT NUMBER

N/A

9. SPONSORING/MONITORING AGENCY NAME(S) AND ADDRESS(ES)

Air Force Office of Scientific Research/NM
875 North Randolph Street
Arlington, VA 22203

10. SPONSOR/MONITOR'S ACRONYM(S)

AFOSR/NM

11. SPONSOR/MONITOR'S REPORT NUMBER(S)

AFRL-SN-HS-JA-2002-0508

12. DISTRIBUTION/AVAILABILITY STATEMENT

UNLIMITED DISTRIBUTION

13. SUPPLEMENTARY NOTES

ESC Public Affairs Clearance #: 02-0508; Published in "Quantum Computing and Quantum Bits in Mesoscopic Systems", A. J. Leggett, B. Ruggiero, and P. Silvestrini eds. Kluwer Academic Plenum Publishers, NY USA, (2003)

14. ABSTRACT

We investigate the properties of Josephson junction triangular prism qubits coupled by mutual inductance to a resonant LC bus. We show how the symmetries of the qubit potential may be used to implement the Duan Cirac Zoller scheme for holonomic quantum computation.

15. SUBJECT TERMS

Josephson junction qubit, geometric gates, holonomic quantum computation.

16. SECURITY CLASSIFICATION OF:			17. LIMITATION OF ABSTRACT	18. NUMBER OF PAGES	19a. NAME OF RESPONSIBLE PERSON
a. REPORT	b. ABSTRACT	c. THIS PAGE			Stanford P. Yukon
U	U	U	UU	12	19b. TELEPHONE NUMBER *(Include area code)*

JOSEPHSON JUNCTION TRIANGULAR PRISM QUBITS COUPLED TO A RESONANT LC BUS

Qubits and gates for a holonomic quantum computer

S. P. Yukon
Air Force Research Laboratory, Electromagnetics Technology Division, Hanscom AFB, MA 01731, USA

Abstract: We investigate the properties of Josephson junction triangular prism qubits coupled by mutual inductance to a resonant LC bus. We show how the symmetries of the qubit potential may be used to implement the Duan Cirac Zoller scheme for holonomic quantum computation.

Keywords: Josephson junction qubit, Geometric gates, Holonomic quantum computation

1. INTRODUCTION

A geometric approach for achieving quantum computation using non-Abelian holonomic gate operations has been recently proposed by Pachos *et al.* [1]. An implementation of (non-Abelian) holonomic quantum computation using a trapped ion quantum computer [2] has subsequently been proposed by L. M. Duan, J. I. Cirac, and P. Zoller (DCZ) [3]. We propose here an alternative physical implementation of holonomic quantum computation based on a previously described quantum computer employing Josephson junction (JJ) triangular prism qubits coupled to a resonant LC bus [4]. For the ion trap system the excitation of different transitions can be distinguished by polarization or by frequency. For qubits based on the symmetric potential well of a JJ triangular prism, symmetric and antisymmetric excitations of prism's two JJ triangles using external magnetic flux take the place of laser pulse polarization. Because the qubit potential well and qubit's interaction with external flux are defined by Bohm Aharonov vector potential integrals around each cell circuit (yielding an Abelian holonomy or Berry phase), the basis for both qubit and gate properties can be said to be of geometric origin.

The DCZ qubits are atomic ions that have the desirable feature that all of the qubits possess identical properties when they are isolated from local environmental perturbations. The JJ qubits that we propose to employ have inherent fabrication errors and no two qubits

Quantum Computing and Quantum Bits in Mesoscopic Systems
Edited by Leggett *et al.*, Kluwer Academic/Plenum Publishers, 2004

will be exactly identical. To overcome this variability, the local microwave rf sources that provide the gate pulses at each qubit need to have their frequencies adjusted to match the transition frequencies needed for that particular qubit. A desirable aspect of holonomic quantum computing for such nonidentical qubits is that once the local rf source frequencies have been adjusted, it is possible to carry out a set of global (or multi-local) logic operations as the holonomic gates depend only on relative phases and amplitudes of the rf gate sources and not on their absolute amplitudes. Because the gate rotation angle for a holonomic gate depends on the solid angle subtended by the closed path in parameter space, holonomic gates should be relatively immune to small random fluctuations in external magnetic flux since the integral of the fluctuations they induce on a closed path should average to zero.

1.1 Josephson junction triangular prism qubits

In Fig. 1 we have sketched the three alternative versions of the flattened JJ prism qubit proposed in Ref. [4]. Of these the four- and five-cell versions have similar properties except that the five-cell version has an extra constraint condition (on the sum of the fluxes through the five cells) that gives rise to unwanted combinations of second-order excitations. Of the two, the simpler four-cell version is thus preferable.

The three- and four-cell versions may be distinguished by the circulating currents in the outer cells when the system is at a potential well minimum. The expressions for the effective one-dimensional potential for both the three- and four-cell versions may be written as $V_r(\chi) = -2\cos(\chi) + r\cos(2\chi)$ (shown in Fig. 3 for $r = 0.675$). The expression for the phase ζ^* of a (dotted) junction at a potential minimum in one of the triangular cells may be written as $\zeta^* = \pm\chi^* + f(\Phi_i)$ where $\pm\chi^*$ are the two minima for $V_r(\chi)$, and $f(\Phi_i)$ represents a function of Φ_is (where Φ_i is the external flux in the ith cell). The circulating current in the left- and right-hand JJ triangular cells at the two minima may be represented as $I_{\mathrm{MEAN}} \pm \Delta I$ (left-hand cell) and $I_{\mathrm{MEAN}} \mp \Delta I$ (right-hand cell). For the three-cell circuit (with $\Phi_s = 0$ defined below) $I_{\mathrm{MEAN}} = 0.415$, $\Delta I = 0.415$ at $r = 1$, and $I_{\mathrm{MEAN}} = 0.65$, $\Delta I = 0.32$ at $r = 0.65$. For the four-cell circuit (with $\Phi_s = 2\Phi_q$ defined below) $I_{\mathrm{MEAN}} = 0.0$, $\Delta I = 0.87$ at $r = 1$, and $I_{\mathrm{MEAN}} = 0.0$, $\Delta I = 0.65$ at $r = 0.65$. The four-cell circuit yields a larger ΔI for gradiometer coupling to a SQUID detector and is therefore the circuit that we choose for the qubit.

The computational basis states for the qubit are taken to be the ground and first excited state of the potential $V_r(\chi)$. Because the ground and first excited states wavefunctions of a symmetric potential are purely symmetric and antisymmetric, respectively, there is an equal probability of the current being in the right- or left-hand JJ triangle. To perform a measurement, a Hadamard gate or a $\pi/2$ Y-rotation on a qubit in one of the basis states will lead to a superposed wavefunction that is centered around the left or right potential well

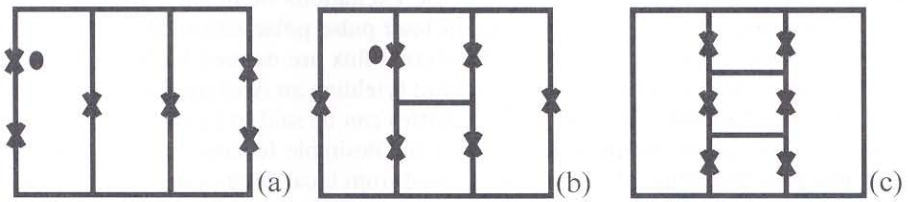

Figure 1. Sketch of three versions of the flattened triangular JJ prism.

minima. This in turn will lead to one of the previously described current patterns that can then be measured by a SQUID detector. A measurement performed without the Hadamard gate would be able to measure symmetric or antisymmetric combinations of the qubit basis states.

While we have used the symmetric properties of the potential $V_r(\chi)$ to define the qubit, we have used the results of Mooij *et al.* with regard to the low inductance properties of the qubit [5–7] and the necessity for suppressing transitions to other charge states [5, 6]. We will not discuss the aspects of coupling the qubit to detectors and the environment here, but the results of Refs [5] and [6] have addressed these issues and are applicable to the qubit proposed here.

The DCZ Hamiltonian employs three ground or metastable states plus a common excited state for each ion qubit. The Hamiltonian in the rotating frame for the jth ion with rf sources for each needed transition turned on, is given by

$$H_j = \hbar\Omega_0|e\rangle_j\langle 0| + \hbar\Omega_1|e\rangle_j\langle 1| + \hbar\Omega_b|e\rangle_j\langle b| + h.c. \tag{1}$$

where Ω_i are the Rabi frequencies for the transition from state $|i\rangle$ to state $|e\rangle$. Transcription of the DCZ holonomic quantum computation scheme to Josephson junction qubits requires: (1) qubits with three degenerate states (in the rotating frame) that couple to a common excited state; (2) a way of exciting each of the three states without exciting the others (and being able to control the amplitude and relative phase of the separate excitation modulation envelopes); and (3) a bus having harmonic oscillator energy levels that can couple to all of the qubits. In the next two sections we demonstrate how this may be accomplished using four-cell JJ prism qubits coupled to a resonant LC bus.

The Hamiltonian (in units of $2E_J$) for the four-cell qubit in Fig. 2, derived in Ref. [4], may be written as

$$\frac{H}{(2E_J)} = -\frac{\partial^2}{\partial\chi^2}2M_\chi - \left\{2\eta_H\cos\left(\frac{\phi_q}{2}\right)\cos\left(\chi+\frac{\phi_a}{2}\right) + \rho\cos(2\chi)\cos(\phi_s+\phi_q)\right\} \tag{2}$$

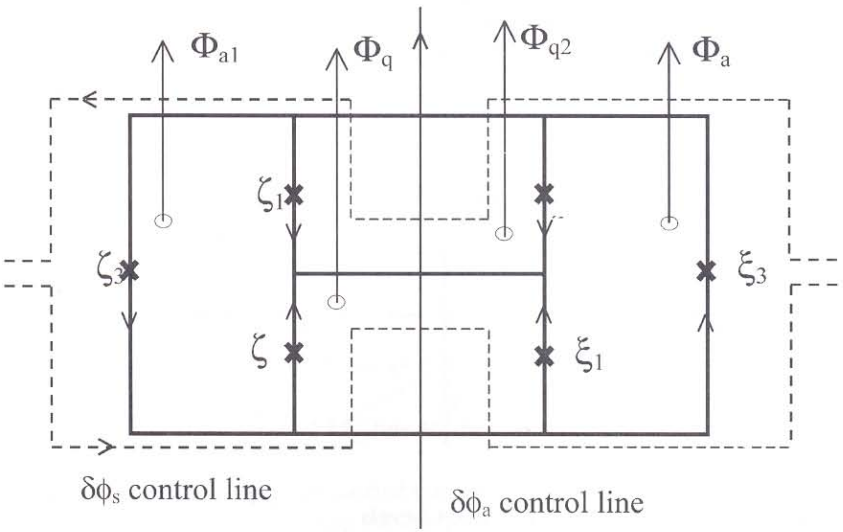

Figure 2. Flattened Josephson junction prism qubit with $\delta\phi_a$ and $\delta\phi_s$ control lines.

where we have defined $\theta = \theta_1 - \phi_r/2$ and $\chi = \psi_1 + (\phi_q - \phi_a)/2$ with $\phi_{q,r} = (\phi_{q1} \pm \phi_{q2})/2$, along with the diagonalizing $\pm$ combinations; $\psi_1 = (\zeta_1 - \zeta_2)/2$, $\psi_2 = (\xi_1 - \xi_2)/2$, $\theta_1 = (\zeta_1 + \zeta_2)/2$, $\theta_2 = (\xi_1 + \xi_2)/2$, as well as $\phi_{s,a} = (\phi_{a1} \pm \phi_{a2})/2$ with the definitions $\phi_{q,s,a} = 2\pi\,\Phi_{q,s,a}/\Phi_0$, $E_J = I_C\Phi_0/2\pi$ and $\Phi_0 = h/2e$. We have used the zero inductance limit Bohm–Aharonov phase constraint equations $\{\zeta_1 - \zeta_2 - \zeta_3 = \phi_{a1}$, $\xi_1 - \xi_2 - \xi_3 = \phi_{a2}$, $-\zeta_1 + \xi_2 = \phi_{q2}$, $\zeta_2 - \xi_1 = \phi_{q1}\}$ for the gauge invariant ζ_i and ξ_i junction phases. For junctions ζ_1, ζ_2, ξ_1, and ξ_2, the junction capacitances and critical currents have been taken equal to C and I_C, respectively. For junctions ζ_3 and ξ_3, the junction capacitances and critical currents have been taken equal to ρC and ρI_C respectively, allowing the mass term M_χ, to be written as $M_\chi = (2E_J)M = (1 + 2\rho)\,(2E_J)/(4(E_C/2))$, with $E_C = e^2/(2C)$. The η_H term comes from the Hartree replacement $\cos(\theta) \rightarrow \langle 0_\theta|\cos(\theta)|0_\theta\rangle \equiv \eta_H$. For the ground state $|0_\theta\rangle$, $\eta_H \approx 1$. In order to introduce the terms of the Hamiltonian that can be utilized for qubit gates, we further divide ϕ_q, ϕ_a, and ϕ_s into constant and small excursion constituents as $\phi_q = \phi_q^0 + \delta\phi_q$, $\phi_a = \phi_a^0 + \delta\phi_a$, and $\phi_s = \phi_s^0 + \delta\phi_s$. We take $\phi_r = 0$ (i.e. no constant or time-varying antisymmetric component of the flux threading the middle two cells).

For this Hamiltonian, the time-independent Schrödinger equation is equivalent to the Whittaker Hill equation, for which exact solutions have been found [8]. The lowest even and odd solutions are denoted by $gc_0(\chi)$, $gs_1(\chi)$, $gc_2(\chi)$, and $gs_3(\chi)$ and are defined in terms of continued fractions. If we identify the computational basis states $\langle\chi|1\rangle$ and $\langle\chi|0\rangle$ with $gc_0(\chi/2)$ and $gs_1(\chi/2)$, the assignment of $gc_2(\chi/2)$ and $gs_3(\chi/2)$ to the DCZ auxiliary states $\langle\chi|e\rangle$ and $\langle\chi|b\rangle$ will allow all of the DCZ one and two qubit holonomic gates to be carried out. The two basis states and auxiliary states are shown in the inset of Fig. 3 along

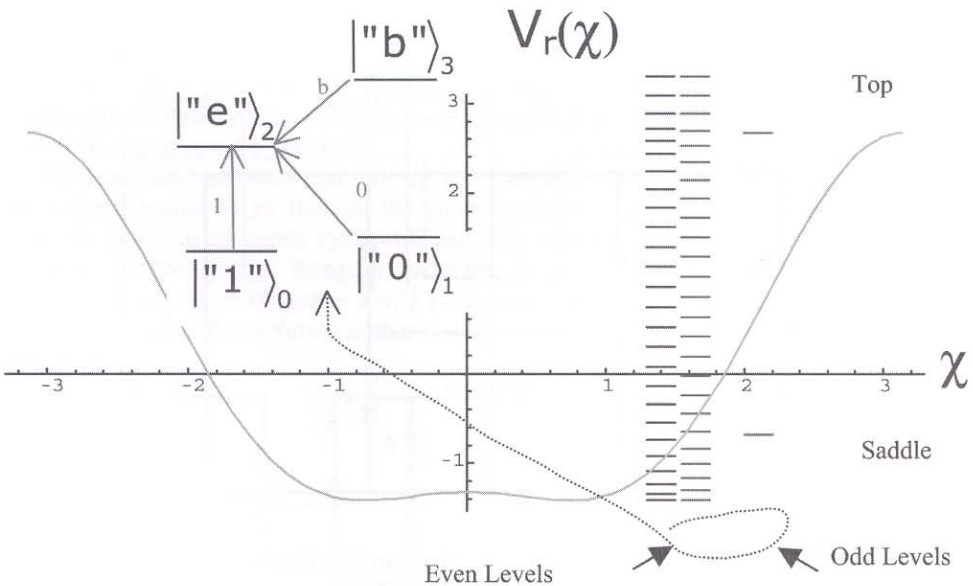

Figure 3. Energy levels and qubit transitions (inset) for $V_r(\chi)$ (in units of $2E_J$) with $r = 0.675$.

with the complete set of bound state levels for the qubit potential of Eq. (2) written as $V_r(\chi) = \cos(\chi + \phi_a/2) - r\cos(2\chi)$ with $r = -\rho\cos(\phi_s^0 + \phi_q^0)/(\eta_H \cos(\phi_q^0/2)) = 0.675$.

Since we have chosen to use the excited states $gc_2(\chi/2)$ and $gs_3(\chi/2)$ as the DCZ auxiliary states, their energy eigenvalues (and that of $gc_4(\chi/2)$, which is a possible transition from $gs_2(\chi/2)$) must lie appreciably below the potential well saddle that separates unit cells in the two-dimensional periodic potential (in order to prevent the excitation of different charge states) [5, 6]. There is a range of values of ϕ_s^0, ϕ_q^0, and η_H for which this is possible. As an example for the choice $r = 0.675$, $M_\chi = 100$, the saddle lies $0.74 \times (2E_J)$ above the potential minimum, while the $gc_4(\chi/2)$ and $gs_3(\chi/2)$ states lie respectively at $0.18 \times (2E_J)$ and $0.12 \times (2E_J)$ above the minimum.

A second requirement for the potential is that the transition frequencies $\omega_{21} = (E_2 - E_1)/\hbar$ and $\omega_{43} = (E_4 - E_3)/\hbar$ be separated by at least $10 \times \Omega_b$, where Ω_b is the Rabi frequency for the $gs_1(\chi/2) \leftrightarrow gc_2(\chi/2)$ transition, in order not to excite the $gs_3(\chi/2) \leftrightarrow gc_4(\chi/2)$ transition.

To model the inclusion of rf forcing and coupling to other qubits, we expand the potential in a power series around $\phi_a^0 = 0$, $\phi_q^0 \neq 0$, and $\phi_s^0 \neq 0$, keeping $\delta\phi_i$ terms up to second order. Physically, the ϕ_q^0 and ϕ_s^0 magnetic flux can be supplied by a uniform external field. The $\delta\phi_a$ excitation can be supplied by a vertical line bisecting the qubit while the $\delta\phi_s$ excitation can be supplied by two symmetric horizontal control lines designed to null or minimize concomitant excitation of $\delta\phi_q$ and $\delta\phi_r$ as shown in Fig. 2 (the wanted $\delta\phi_q$ excitations will come from the bus). The rf excitations $\delta\phi_{a,s}$ are tuned to the transition frequency between $|e\rangle$ and $|0\rangle$, $|1\rangle$, or $|b\rangle$. Thus the full expression for $\delta\phi_a$ for the $b \leftrightarrow e$ transition is thus given by

$$\delta\phi_a^{\langle e,b\rangle} = \delta\phi_a^{(b)}(t)e^{i(E_e - E_b)t/\hbar + i\varphi_b} \tag{3}$$

where $\delta\phi_a^{(b)}(t)$ is the adiabatically varying modulation of the rf pulse envelope. The time varying phase $\varphi_b(t)$ may be introduced as a frequency modulation of the carrier at the transition frequency $(E_e - E_b)/\hbar$ with the FM pulse frequency given by $\omega_{eb}(t) = (E_e - E_b)/\hbar + d\varphi_b(t)/dt$.

The Hamiltonian for the jth qubit in the rotating frame with all rf sources on, may thus be expressed as the DCZ Hamiltonian of Eq. (1) with the Rabi frequencies for the three needed transitions given by

$$\Omega_0 = \eta_H\langle 0|\sin(\chi)|e\rangle\cos(\phi_q^0/2)\delta\phi_a^{(0)} \tag{4a}$$

$$\Omega_1 = \rho\langle 1|\cos(2\chi)|e\rangle\sin(\phi_s^0 + \phi_q^0)\delta\phi_s^{(1)} \tag{4b}$$

and

$$\Omega_b = \eta_H\langle b|\sin(\chi)|e\rangle\cos(\phi_q^0/2)\delta\phi_a^{(b)} \tag{4c}$$

1.2 Coupling the resonant LC bus to the qubits

To enable two-qubit gates to be carried out, each of the qubits is coupled to a resonant LC bus by mutual inductance coupling between a loop in the bus and the two inner cells of the qubit as shown in Fig. 5. The bus is based on the trapped ion bus scheme of Refs. [3, 9, 10] and is similar to the resonant LC bus coupling of qubits in Refs. [11–13]. The

operators for flux and charge in an LC oscillator with resonant frequency $\omega = 1/\sqrt{LC}$, can be written in terms of creation and annihilation operators $\{\mathbf{a}^+, \mathbf{a}\}$ as

$$\mathbf{\Phi} = \sqrt{\frac{\hbar L\omega}{2}}(\mathbf{a} + \mathbf{a}^+), \quad Q = i\sqrt{\frac{\hbar}{2L\omega}}(\mathbf{a} - \mathbf{a}^+) \tag{5}$$

If there are N qubits coupled to the bus, and a fraction $f_Q\mathbf{\Phi}$ is available for coupling to the qubits, the amount of flux coupled to each qubit will be $f_Q\mathbf{\Phi}/N$. The second-order terms in the Hamiltonian expansion will then yield interaction terms for even–even (or odd–odd) transitions $\hat{\Omega}_1^j\sigma_{j1}^0(\mathbf{a} + \mathbf{a}^+)$ and even–odd transitions $\hat{\Omega}_0^j\sigma_{j0}^0(\mathbf{a} + \mathbf{a}^+)$ and $\hat{\Omega}_b^j\sigma_{jb}^0(\mathbf{a} + \mathbf{a}^+)$, where

$$\sigma_{j\mu}^{\varphi_\mu} = e^{i\varphi_\mu}|e\rangle_j\langle\mu| + h.c. \text{ Hermitian conjugate} \tag{6}$$

and

$$\hat{\Omega}_0^j = -\left(\frac{\eta_H}{2}\right)\sin\left(\frac{\phi_q^0}{2}\right)\langle 0|\sin(\chi)|e\rangle 2\pi f_q \frac{\sqrt{\hbar L\omega/2}}{(N\Phi_0)\delta\phi_a^{(0)}} \tag{7a}$$

$$\hat{\Omega}_1^j = \rho\cos(\phi_s^0 + \phi_q^0)\langle 1|\cos(2\chi)|e\rangle 2\pi f_q \frac{\sqrt{\hbar L\omega/2}}{(N\Phi_0)\delta\phi_s^{(1)}} \tag{7b}$$

$$\hat{\Omega}_b^j = -\left(\frac{\eta_H}{2}\right)\sin\left(\frac{\phi_q^0}{2}\right)\langle a|\sin(\chi)|e\rangle 2\pi f_q \frac{\sqrt{\hbar L\omega/2}}{(N\Phi_0)\delta\phi_a^{(b)}} \tag{7c}$$

Adopting the Sørensen and Mølmer [5, 6] bichromatic bus scheme used by DCZ, which requires only virtual bus excitations, the effective Hamiltonian for a pair $\{j, k\}$ of qubits coupled by the resonant LC bus may be written as

$$\frac{H_{j,k}}{2E_J} = \left(\frac{1}{\delta}\right)\left[\left(\frac{\delta}{\delta_0}\right)|\hat{\Omega}_0^j||\hat{\Omega}_0^k|\sigma_{j0}^{\varphi_0}\sigma_{k0}^{\varphi_0} - |\hat{\Omega}_1^j||\hat{\Omega}_1^k|\sigma_{j1}^{\varphi_1}\sigma_{k1}^{\varphi_1} + |\hat{\Omega}_b^j||\hat{\Omega}_b^k|\sigma_{jb}^{\varphi_b}\sigma_{kb}^{\varphi_b}\right] \tag{8}$$

This expressions differs from those in DCZ and Refs. [5, 6] due to the fact that we have taken into account the slightly different parameters of each qubit, and have allowed for a third detuning frequency offset δ_0 in addition to the DCZ frequency offset δ.

The total capacitance C will consist of the capacitance between the wires forming the bus and any additional capacitance added. The bus frequency $\omega = 1/\sqrt{LC}$ is chosen to avoid direct excitation of transitions in the qubit and to optimize the number of qubits in the system. To remain within the quasi-static limit, the maximum extent of the bus is $\sim 0.1\lambda_s$, where λ_s is the substrate wavelength. Assuming a bus frequency of 3 GHz, and a *substrate refractive index* $n_s = 3.0$ yields $\lambda_s/10 = 0.33$ mm. Assuming $(2E_J)/h = 200$ GHz, with $r = 0.675$, $M_\chi = 100$ the expressions (4c) and (7c) with $\delta\phi_a = 0.001 \times 2\pi$ yield $\Omega_b/2\pi = 0.152$ GHz and $\hat{\Omega}_b^j/2\pi = 0.627/\sqrt{N}$ MHz. The Rabi frequencies for two-qubit gates given in Eq. (8) may be increased from this value by taking the offset frequencies δ and δ_0 to be small fractions of $\hat{\Omega}_b^j$, and by choosing n such that the rf frequency $\omega_{\text{rf}} = (E_2 - E_1)/h + n \cdot \omega$ is distant from any allowed transition

frequency so that the value of $\delta\phi_a$ could be increased. An example would be to choose n such that $\omega_{\rm rf} \approx (E_7 - E_1)/\hbar$.

We note that by setting $\phi_q = 0$, the middle cells in Fig. 1 may be eliminated and their junctions combined. The bus for these two-cell versions should then be moved to the right (or left) cell. From Eqs (4) and (7) we see that for Fig. 1(b), all one-qubit terms would survive but only the even two-qubit term (7b) would survive for $\phi_q = 0$. This would still allow a universal set of gates to be formed but without the extra degree of control from the even–odd transition terms (7a) and (7c). The two-cell version of Fig. 1(a) would have similar losses. For Fig. 1(c), all even transition terms vanish [14]. For one-qubit gates, an even term could be fashioned for $|1\rangle \rightarrow |e\rangle$ by using second-order odd transitions since the energy denominator for the intermediate state transition $|1\rangle \rightarrow |0\rangle$ is small.

1.3 Non-Abelian holonomic gates

The basic set of DCZ single qubit gates $U_1^{(j)} = e^{i\phi_1|1_j\rangle\langle 1_j|}$, $U_Y^{(j)} = e^{i\phi_Y\sigma_y^{(j)}}$, and the two-qubit gate $U_{11}^{(j,k)} = e^{i\phi_{11}|1_j,1_k\rangle\langle 1_j,1_k|}$ are sufficient for all of the operations needed to carry out holonomic quantum computations. The DCZ Berry phases ϕ_1, ϕ_Y, and ϕ_{11}, are given by their implicit dependence on θ and φ as:

$$\phi_1 = -\frac{1}{2}\oint \sin(\theta)\, d\theta\, d\varphi \tag{9}$$

with

$$\Omega_0 = 0, \quad \Omega_1 = -\Omega' \sin\left(\frac{\theta}{2}\right) e^{i\varphi}, \quad \Omega_b = \Omega'' \cos\left(\frac{\theta}{2}\right)$$

$$\phi_Y = \oint \sin(\theta)\, d\theta\, d\varphi \tag{10}$$

with

$$\Omega_0 = \Omega \sin(\theta)\cos(\varphi), \quad \Omega_1 = \Omega' \sin(\theta)\sin(\varphi), \quad \Omega_b = \Omega''\cos(\theta)$$

with $\Omega = \Omega' = \Omega''$ and

$$\phi_{11} = -\frac{1}{2}\oint \sin(\theta)\, d\theta\, d\varphi \tag{11}$$

with

$$\Omega_0 = 0, \quad \frac{|\hat{\Omega}_1^j \hat{\Omega}_1^k|}{|\hat{\Omega}_b^j \hat{\Omega}_b^k|} = \tan\left(\frac{\theta}{2}\right), \quad \varphi_1 - \varphi_b = \frac{\varphi}{2}$$

The minimal set of gates for quantum computation (two single-qubit gates and one two-qubit gate) must form a noncommuting set, which implies that their geometric phases must be generated by non-Abelian holonomies [1]. The computational basis during an adiabatic evolution cycle rotates into "dark" states that maintain zero eigenvalues. An example of dark states for the $U_Y^{(j,k)}$ gate Hamiltonian would be $|D_{Y1}\rangle = \cos(\theta)(\cos(\varphi)|0\rangle_j + \sin(\varphi)|1\rangle_j) - \sin(\varphi)|b\rangle_j$ and $|D_{Y2}\rangle = \cos(\varphi)|0\rangle_j - \sin(\varphi)|1\rangle_j$. Since the gate Hamiltonians

have zero eigenvalues for these states, there is no dynamical phase contribution from the gates to the computational basis states [1].

Using expressions for the geometric phase in [1], the DCZ set can be completed with the single-qubit X rotation and two-qubit $X_{\alpha\beta,\alpha'\beta'}$ and $Y_{\alpha\beta,\alpha'\beta'}$ rotations where σ_x and σ_y are replaced by $\{|\alpha\beta\rangle\langle\alpha'\beta'| + |\alpha\beta\rangle\langle\alpha'\beta'|\}$ and $\{-i|\alpha\beta\rangle\langle\alpha'\beta'| + i|\alpha'\beta'\rangle\langle\alpha\beta|\}$, respectively, and $|\alpha\beta\rangle$ (and $|\alpha'\beta'\rangle$) is one of the two-qubit states $\{|0_j0_k\rangle, |0_j1_k\rangle, |1_j0_k\rangle, |1_j1_k\rangle\}$. The expression for the X rotation is given by $U_X^{(j)} = e^{i\phi_x\sigma_x^{(j)}}$ where

$$\phi_X = \oint \sin(\theta)\, d\theta\, d\varphi \tag{12}$$

with

$$\Omega_0 = \Omega\sin(\theta)\cos(\varphi), \quad \Omega_1 = \Omega'\sin(\theta)\sin(\varphi)e^{i\pi/2}, \quad \Omega_b = \Omega''\cos(\theta)$$

For $Y_{\alpha\beta,\alpha'\beta'}$ rotation the two-qubit Hamiltonian can be written as

$$H_{j,k}^{Y_{\alpha\beta,\alpha'\beta'}} = \left(\frac{1}{\delta}\right)\left[\left(\frac{\delta}{\delta_0}\right)|\hat{\Omega}_{\alpha\beta}^{j}||\hat{\Omega}_{\alpha\beta}^{k}|\sigma_{j\alpha}^{\varphi_{\alpha\beta}}\sigma_{k\beta}^{\varphi_{\alpha\beta}} - |\hat{\Omega}_{\alpha'\beta'}^{j}||\hat{\Omega}_{\alpha'\beta'}^{k}|\sigma_{j\alpha'}^{\varphi_{\alpha'\beta'}}\sigma_{k\beta'}^{\varphi_{\alpha'\beta'}}\right.$$
$$\left. + |\hat{\Omega}_b^{j}||\hat{\Omega}_b^{k}|\sigma_{jb}^{\varphi_b}\sigma_{kb}^{\varphi_b}\right] \tag{13}$$

The $Y_{\alpha\beta,\alpha'\beta'}$ rotation is then given by

$$U_{Y_{\alpha\beta,\alpha'\beta'}}^{(j,k)} = e^{i\phi_{Y_{\alpha\beta,\alpha'\beta'}}(-i|\alpha_j,\beta_k\rangle\langle\alpha'_j,\beta'_k| + i|\alpha'_j,\beta'_k\rangle\langle\alpha_j,\beta_k|)}$$

with

$$\phi_{Y_{\alpha\beta,\alpha'\beta'}} = \oint \sin(\theta)\, d\theta\, d\varphi \quad \text{and} \quad \Omega_{\alpha\beta} = \Omega\sin(\theta)\cos(\varphi), \tag{14}$$

with

$$\Omega_{\alpha'\beta'} = \Omega'\sin(\theta)\sin(\varphi), \quad \Omega_b = \Omega''\cos(\theta)$$

The $X_{\alpha\beta,\alpha'\beta'}$ rotation can be similarly derived following the pattern of the single-qubit X and Y rotations.

1.4 Fault tolerance of U_1 and U_{11} and U_Y and $U_{Y_{\alpha\beta,\alpha'\beta'}}$ holonomic gates

Assuming that it will not be possible to adjust the three microwave sources at each qubit to obtain equal basic Rabi frequencies Ω for the three needed transitions, we have looked at the effect of unequal basic Rabi frequencies $\{\Omega, \Omega', \Omega''\}$ on the value of the resulting gate rotation angle. We define an "input" gate rotation angle ϕ_{in} as the Berry angle given in Eqs (9), (10), or (11) for a perfectly adjusted system with a three-step pulse sequence: $\{\theta = 0 \to \pi/2,\ \varphi = 0\}$, $\{\theta = \pi/2,\ \varphi = 0 \to \varphi_{\text{final}}\}$, $\{\theta = \pi/2 \to 0,\ \varphi = \varphi_{\text{final}}\}$. The pulse envelope used is $\theta(t) = \hat{\theta}(\tanh(\lambda(t + t_0)) - \tanh(\lambda(t - t_0)))/2$, $\varphi(t) = \hat{\varphi}(\tanh(\lambda t + 1)/2$, with $\lambda = 1/2$, $t_0 = 20$, $\hat{\theta} = \pi/2$, $\Omega = \Omega_\lambda = 2\pi$. The gate rotations presented below are calculated in the restricted Hilbert space $\mathcal{H}_0 = \{|0\rangle, |1\rangle, |e\rangle, |b\rangle\}$. In Fig. 4(a) we have plotted the resulting gate rotation angle ϕ_{out} for the U_1 gate for $\{\Omega, \Omega', \Omega''\} = \Omega_\lambda\{0, 1.0, 1.0\}$, $\Omega_\lambda\{0, 1.0, 1.2\}$, and $\Omega_\lambda\{0, 1.0, 1.4\}$. Since all of the gate rotation angles lie on a straight line for a given set of basic Rabi

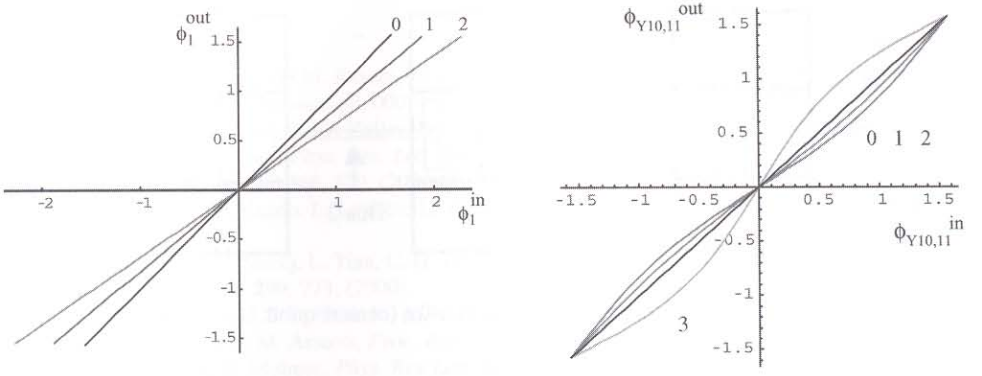

Figure 4. (a) Output vs. input rotation angle for basic Rabi frequency error sets 0, 1, 2; (b) Output vs. input rotation angle for basic Rabi frequency error sets 0, 1, 2, 3.

frequencies, measurement of a single pair of input and output rotation angles will then determine the needed input angle for any desired output rotation angle. The behavior of all gates like U_{11} that have $\Omega_0 = 0$ will be similar.

In Fig. 4(b) we have plotted the output rotation angle for the $U_{Y_{10,11}}$ gate for $\{\Omega, \Omega', \Omega''\} = \Omega_\lambda\{1.0, 1.0, 1.0\}$, $\Omega_\lambda\{1.0, 1.22, 0.83\}$, $\Omega_\lambda\{1.00, 1.44, 0.66\}$, and $\Omega_\lambda\{1.00, 0.66, 1.34\}$. For this gate all of the output rotation angles for a given set of basic Rabi frequencies lie on a 45° rotated sine curve. Measurement of a single pair of input and output rotation angles can then determine the needed input angle for any desired output rotation angle. The behavior of all gates like U_X, U_Y, and $U_{X_{\alpha\beta,\alpha'\beta'}}$ that have adiabatic envelopes similar to Eq. (10) will have behavior similar to that of $U_{Y_{\alpha\beta,\alpha'\beta'}}$. Unlike the U_{11} and U_1 gates, there are also two points at $\pm\pi/2$ where the output rotation angle perfectly matches the input rotation angle. Thus any of the gates U_X, U_Y, $U_{X_{\alpha\beta,\alpha'\beta'}}$, or $U_{Y_{\alpha\beta,\alpha'\beta'}}$ at rotation angle $\pm\pi/2$ will be fault tolerant with respect to microwave pulse amplitude errors. Investigation of the fault tolerance properties of gates when the Hilbert space is not restricted to $\mathcal{H}_0$ requires optimizing the potential, the resonant pulses, and bus parameters to minimize leakage out of $\mathcal{H}_0$, and will be addressed in a future paper.

1.5 Connecting buses into a network

It is also possible to connect groups of buses in an open branching network as first described in Ref. [4]. To transcribe this feature to the holonomic qubits and gates described above requires distinguishing a particular qubit (or qubits) that is to be assigned the sole task of transferring gate excitations from one bus to a second and vice versa. This is shown schematically in Fig. 5. Since the $U_{Y_{10,11}}$ is fault tolerant at rotation angle $\pm\pi/2$, we shall employ it to connect buses and define it as

$$U_{CY_{j,k}}(\pm) = \{|0_j0_k\rangle\langle 0_j0_k| + |0_j1_k\rangle\langle 0_j1_k| \mp |1_j1_k\rangle\langle 1_j0_k| \pm |1_j0_k\rangle\langle 1_j1_k|\} \qquad (15)$$

To carry out a two-qubit $U_{CY_{j,k}}(\pm)$ gate between a control qubit j on bus 1 and a target qubit k on bus 2 via the common transfer qubit t (assumed to be in its ground state), it is necessary

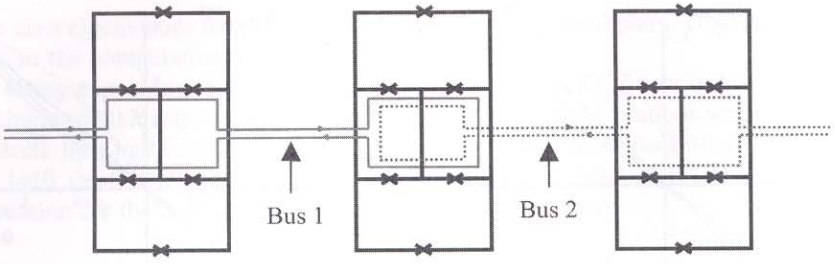

Figure 5. Schematic of two coupled buses and transfer (center) qubit.

to first carry out a $U_{CY_{j,t}}(-)$ gate with qubit j the control qubit and qubit t the target qubit. A second $U_{CY_{t,k}}(-)$ gate with qubit t the control and qubit k the target and a final $U_{CYj,t}(-)$ gate with qubit j the control qubit and qubit t the target qubit achieve the desired result with control qubit t returned to its original ground state. While they are not perfectly fault tolerant, three control-not gates, between (j, t), (t, k), and (j, t) would also have the overall effect of a control-not between j and k with t reset to its original ground state.

To carry out a control-y over a number of buses, it is necessary to first carry out a sequence of $U_{CY_{i,j}}(-)$ starting from the control qubit, through all of the intervening transfer qubits to the target qubit, followed by a final sequence of $U_{CY_{i,j}}(-)$ from the original qubit to the last transfer qubit in order to reset the transfer qubits to their original ground states. The sequence involving two transfer qubits would thus be $U_{CY_{i,j}}(-)$ between (j, t_1), (t_1, t_2), (t_2, k) followed by resetting transfer qubits with $U_{CY_{i,j}}(-)$ applied to (t_1, t_2) and (j, t_1). The maneuvers described in the preceding paragraph may be chained across as many coupled buses as required (given an environment where perfect coherence is possible). This allows open branching networks of coupled buses to be formed, enlarging the possible number of interacting qubits in a single quantum computer.

2. CONCLUSIONS

We have shown that it is possible to design a system comprised of Josephson junction prism qubits coupled inductively to a resonant LC bus that is capable of carrying out holonomic quantum computations. The effective Hamiltonian is zero throughout an entire computation, so there is no dynamical evolution of the system. In the restricted Hilbert space $\mathcal{H}_0$, one- and two-qubit X and Y rotation gates are shown to be tolerant of pulse amplitude errors for rotation angles of $\pm\pi/2$. The behavior of one- and two-qubit gates at arbitrary rotation angles, when pulse amplitude errors are present, can be predicted if one measurement can be made to determine an appropriate input/output curve.

Acknowledgements

The author appreciates helpful conversations with Alexey Ustinov, Jeffrey Yepez, Farrukh Abdumalikov, and Jim Ernstmeyer. This work was carried out with support from Air Force Office of Scientific Research AFOSR.

REFERENCES

[1] J. Pachos, P. Zanardi, and M. Rasetti, *Phys. Rev.* **A61**, 010305(R) (2000), J. Pachos Preprint http://www.xxx.lanl.gov/abs/quant-ph/0007110.
[2] L.-M. Duan, J. I. Cirac, and P. Zoller, *Science*, **292**, 1695 (2001).
[3] J. I. Cirac and P. Zoller, *Phys. Rev. Lett.* **74**, 4091 (1995).
[4] S. P. Yukon, *Physica* **C 368**, 320, (2002).
[5] J. E. Mooij, T. P. Orlando, L. Levitov, L. Tian, C. H. van der Wal, and S. Lloyd, *Science* **285**, 1036 (1999).
[6] T. P. Orlando, J. E. Mooij, L. Tian, C. H. van der Wal, L. S. Levitov, S. T. P. Orlando, S. Lloyd, and J. E. Mooij, *Science* **290**, 773, (2000).
[7] D. S. Crankshaw and T. P. Orlando, *IEEE Trans. Appl. Sup.* **11**, 1006 (2001).
[8] K. M. Unwin and F. M. Arscott, *Proc. Roy Soc. Edinb.* **71**, 28 (1971).
[9] A. Sørensen and K. Mølmer, *Phys. Rev Lett.* **82**, 1971 (1999).
[10] A. Sørensen and K. Mølmer, *Phys. Rev Lett.* **82**, 1835 (1999).
[11] Y. Makhlin, G. Schön, and A. Shnirman, *J. Low Temp. Phys.* **118**, 751 (2000).
[12] Y. Makhlin, G. Schön, and A. Shnirman, *Rev. Mod. Phys.* **73**, 357 (2001).
[13] O. Buisson and F. W. Hekking, in *Macroscopic Quantum Coherence and Quantum Computing* (Dordrecht, Kluwer Academic), p. 137 (2001).
[14] Mooij, J. E., these proceedings MQC2 2002.